Supported Iridium Cluster Catalysts for Propene Hydrogenation: Identification by X-Ray Absorption Spectra Measured During Catalysis

Ghansham Panjabi, Andrew M. Argo, and Bruce C. Gates*[a]

Abstract: Supported metal carbonyl clusters, $[Ir_4(CO)_{12}]/\gamma$-Al_2O_3, $[Ir_6(CO)_{15}]^{2-}/\gamma$-$Al_2O_3$, and $[HIr_4(CO)_{11}]^-$/MgO, were treated in He to prepare supported metal clusters modeled as Ir_4/γ-Al_2O_3, Ir_6/γ-Al_2O_3, and Ir_4/MgO. The samples were characterized by infrared and extended X-ray absorption fine structure (EXAFS) spectroscopy, with the EXAFS data obtained for samples at liquid nitrogen temperature under vacuum and at 298 K in a flow-through cell in the presence of a) N_2, b) H_2, c) propene, and d) H_2 + propene mixtures; the mixtures underwent catalytic hydrogenation during the measurements. The results indicate that the cluster frames were essentially unchanged under the various conditions. The Ir_4 and Ir_6 clusters are identified as the catalytically active species.

Keywords: catalysts · clusters · EXAFS spectroscopy · hydrogenations · iridium

Introduction

The metals in practical noble-metal catalysts are almost always clusters or particles dispersed on surfaces of porous metal oxide supports. As the clusters or particles are both extremely small and nonuniform, it is difficult to identify the structures responsible for catalysis. Consequently, attempts have been made to synthesize nearly uniform supported metal clusters from precursor metal carbonyl clusters by deposition or surface-mediated formation of the precursors, for example, $[Ir_4(CO)_{12}]$ or $[Ir_6(CO)_{15}]^{2-}$, followed by decarbonylation with retention of the metal frame.[1, 2]

Open questions have to do with how the structures of the cluster frames depend on adsorbed reactant ligands and how these structures may change during catalysis. Because the structures of supported metal clusters—provided they are nearly uniform—may be determined relatively precisely by extended X-ray absorption fine structure (EXAFS) spectroscopy,[1, 3] and because this technique is well-suited to investigation of catalysts in the working state,[4] provided that the temperature is not too high, we have now applied it to characterize supported metal clusters, approximated as Ir_4 and Ir_6 on the supports γ-Al_2O_3 and MgO, in the presence of H_2, propene, and mixtures of H_2 + propene undergoing catalytic hydrogenation. The data lead to the identification of Ir_4 and Ir_6 as catalytically active species and give evidence of the stability of the clusters under mild reaction conditions (298 K and 1 bar).

[a] Prof. B. C. Gates,[+] G. Panjabi, A. M. Argo
Department of Chemical Engineering and Materials Science
University of California, Davis, CA 95616 (USA)
Fax: (+1) 530-752-1031
E-mail: bcgates@ucdavis.edu

[+] Current address:
Prof. B. C. Gates
Institut für Physikalische Chemie, LMU München
Butenandtstrasse 5–13 (Haus E), 81377 München (Germany)

Results

Synthesis and decarbonylation of supported metal clusters: The precursors, $[Ir_4(CO)_{12}]$ and $[Ir(CO)_2(acac)]$, and the supports, γ-Al_2O_3 and MgO, were used to synthesize the following supported metal carbonyl clusters, which are catalyst precursors: $[Ir_4(CO)_{12}]/\gamma$-Al_2O_3, $[HIr_4(CO)_{11}]^-$/MgO, and $[Ir_6(CO)_{15}]^{2-}/\gamma$-$Al_2O_3$. These samples were decarbonylated by heating in flowing He to form the supported clusters approximated as Ir_4/γ-Al_2O_3, Ir_4/MgO, and Ir_6/γ-Al_2O_3. The preparation and characterization by infrared and EXAFS spectroscopy are summarized below.

Infrared spectra of supported metal carbonyl clusters: $[Ir_4(CO)_{12}]/\gamma$-Al_2O_3 and $[HIr_4(CO)_{11}]^-$/MgO were prepared by bringing solutions of $[Ir_4(CO)_{12}]$ in contact with each of the calcined (673 K) metal oxide powders in an *n*-pentane slurry, followed by overnight stirring, and removal of the solvent by evacuation. Infrared spectra of the resulting solids match those reported,[1, 5, 6] which are consistent with the formation of $[Ir_4(CO)_{12}]/\gamma$-Al_2O_3 and $[HIr_4(CO)_{11}]^-$/MgO. Treatment in He at 573 K for 2 h led to removal of the ν_{CO} bands, indicating complete decarbonylation.

 © WILEY-VCH Verlag GmbH, D-69451 Weinheim, 1999 0947-6539/99/0508-2417 $ 17.50+.50/0

$[Ir_6(CO)_{15}]^{2-}/\gamma$-$Al_2O_3$ was prepared by surface-mediated organometallic synthesis.[7] After adsorption of $[Ir(CO)_2$-(acac)] on uncalcined γ-Al_2O_3, the sample was treated in flowing CO at 1 bar and 373 K for 10 h, with the final infrared spectrum matching that of $[Ir_6(CO)_{15}]^{-2}/\gamma$-$Al_2O_3$, the product of reductive carbonylation; details are presented elsewhere.[2] Treatment in He at 573 K for 2 h led to complete decarbonylation, as shown by removal of the ν_{CO} bands; the results match those reported.[2]

EXAFS spectra: The EXAFS data, collected with the samples under vacuum (1.3×10^{-5} mbar) at approximately liquid nitrogen temperature, were analyzed on the basis of data characterizing reference compounds (Table 1). Details of the analysis are presented in Table 1 and in the section below entitled EXAFS data analysis.

Table 1. Crystallographic data characterizing the reference compounds and Fourier transform ranges used in the EXAFS data analysis.[a]

	Crystallographic data			Fourier transform		
	Shell	N	R [Å]	Δk [Å^{-1}]	Δr [Å]	n
Pt foil	Pt–Pt	12	2.77	1.9–19.8	1.9–3.0	3
$Na_2Pt(OH)_6$	Pt–O	6	2.05	1.4–17.7	0.5–2.0	3
$[Ir_4(CO)_{12}]$	Ir–C	3	1.87	2.8–16.5	1.1–2.0	3
	Ir–O*	3	3.01	2.8–16.5	2.0–3.3	3
IrAl alloy	Ir–Al[b]	8	2.58	2.7–12.0	1.0–3.0	3

[a] Notation: N, coordination number characterizing absorber-backscatterer pair; R, distance; Δk, limits used for forward Fourier transformation (k is the wave vector); Δr, limits used for shell isolation (r is distance); n, power of k used for Fourier transformation. [b] After subtraction of Ir–Ir contributions: $N = 6$, $r = 2.98$ Å, $\Delta\sigma^2 = -0.001$ Å^2 ($\Delta\sigma^2$ is the Debye-Waller factor), $\Delta E_0 = -3.3$ eV (ΔE_0 is the inner potential correction). A theoretical Ir–Al EXAFS function was calculated with the FEFF program[8] and adjusted to agree with limited Ir–Al reference data obtained as described above for use of a larger interval in k space for fitting the iridium data.[9]

The EXAFS parameters characterizing $[Ir_4(CO)_{12}]/\gamma$-Al_2O_3, $[HIr_4(CO)_{11}]^-$/MgO, and $[Ir_6(CO)_{15}]^{2-}/\gamma$-$Al_2O_3$ are summarized in Table 2. For example, the structural parameters characterizing $[Ir_4(CO)_{12}]/\gamma$-Al_2O_3 include a first-shell Ir–Ir coordination number of 3.2 with an Ir–Ir distance of 2.66 Å, nearly matching the corresponding values for crystalline $[Ir_4(CO)_{12}]$ (3.0 and 2.69 Å, respectively[10]). The EXAFS data also indicate several Ir-low-Z scatterer contributions, including Ir–CO, with approximately 3 CO groups per Ir atom.

Table 2. EXAFS results at the Ir L_{III} edge characterizing metal carbonyl clusters formed from organometallic precursors on metal oxides at liquid nitrogen temperature and 1.3×10^{-5} mbar.[a]

Supported metal catalyst			EXAFS parameters				
Precursor metal carbonyl	Support	Shell	N	R [Å]	$10^3 \times \Delta\sigma^2$ [Å^2]	ΔE_0 [eV]	EXAFS reference
$[Ir_4(CO)_{12}]$	γ-Al_2O_3	Ir–Ir	3.2	2.66	4.2	0.9	Pt–Pt
		Ir–CO					
		Ir–C	2.9	1.86	3.2	3.3	Ir–C*
		Ir–O*	3.0	2.89	1.8	7.1	Ir–O*
		Ir–$O_{support}$	0.7	2.29	3.5	2.7	Pt–O*
$[Ir(CO)_2(acac)]$	γ-Al_2O_3	Ir–Ir	4.2	2.74	2.4	0.2	Pt–Pt
		Ir–CO					
		Ir–C_b	1.0	2.06	−1.5	−1.8	Ir–C*
		Ir–C_t	2.1	1.85	1.5	5.1	Ir–C*
		Ir–O*	1.8	3.24	−0.7	−5.3	Ir–O*
		Ir–Al	0.2	1.47	5.6	19.1	Ir–Al
$[Ir_4(CO)_{12}]$	MgO	Ir–Ir	3.0	2.69	5.2	14.3	Pt–Pt
		Ir–CO					
		Ir–C	2.87	1.89	9.2	−2.7	Ir–C*
		Ir–O*	2.35	2.95	5.4	3.6	Ir–O*
		Ir–$O_{support}$	0.24	2.13	−5.3	5.2	Pt–O

[a] Notation: N, coordination number; R, distance between absorber and backscatterer atom; $\Delta\sigma^2$, Debye-Waller factor; ΔE_0, inner potential correction; O* = carbonyl oxygen; subscripts b and t, bridging and terminal.

Similarly, the EXAFS data are consistent with the presence of $[HIr_4(CO)_{11}]^-$ on MgO[11] and $[Ir_6(CO)_{15}]^{2-}$ on γ-Al_2O_3.[12] The data characterizing $[Ir_6(CO)_{15}]^{2-}/\gamma$-$Al_2O_3$ indicate both bridging and terminal CO ligands.[2]

EXAFS results characterizing the decarbonylated metal clusters are summarized in Table 3 for the samples represented as Ir_4/γ-Al_2O_3, Ir_4/MgO, and Ir_6/γ-Al_2O_3. The data are consistent with the full removal of the carbonyl ligands as a result of the decarbonylation treatments,[1, 2, 6] with retention of the metal frames, as indicated by the virtually unchanged Ir–Ir coordination numbers.

Table 3. EXAFS results at the Ir L_{III} edge characterizing decarbonylated supported metal clusters at liquid nitrogen temperature and 1.3×10^{-5} mbar.[a]

Cluster/support modeled as	Catalyst Precursor/support + treatment	Shell	N	R [Å]	$10^3 \times \Delta\sigma^2$ [Å^2]	ΔE_0 [eV]	EXAFS reference
Ir_4/γ-Al_2O_3	$Ir_4(CO)_{12}/\gamma$-Al_2O_3 + He, 573 K, 2 h	Ir–Ir	3.3	2.67	4.2	−0.6	Pt–Pt
		Ir–$O_{support}$					
		Ir–O_s	1.1	2.17	1.0	−15.2	Pt–O
		Ir–O_l	0.7	2.69	−2.7	−9.9	Pt–O
		Ir–Al	0.3	1.78	5.0	5.5	Ir–Al
Ir_6/γ-Al_2O_3	$Ir(CO)_2(acac)/\gamma$-Al_2O_3 + He, 573 K, 2 h	Ir–Ir	4.0	2.68	3.3	0.9	Pt–Pt
		Ir–$O_{support}$					
		Ir–O_s	0.5	2.18	−3.2	−6.3	Pt–O
		Ir–O_l	1.3	2.66	3.3	−4.7	Pt–O
		Ir–Al	0.2	1.53	−3.9	−4.9	Ir–Al
Ir_4/MgO	$Ir_4(CO)_{12}$/MgO + He, 573 K, 2 h	Ir–Ir	3.0	2.67	4.2	−0.6	Pt–Pt
		Ir–$O_{support}$					
		Ir–O_s	1.3	2.15	1.0	15.2	Pt–O
		Ir–O_l	0.5	2.69	5.0	−9.9	Pt–O

[a] Notation as in Table 2. Ir–O_s = short and Ir–O_l = long Ir–O contribution.

© WILEY-VCH Verlag GmbH, D-69451 Weinheim, 1999
0947-6539/99/0508-2418 $ 17.50+.50/0 *Chem. Eur. J.* **1999**, *5*, No. 8

EXAFS spectra characterizing catalysts in the presence of adsorbates: EXAFS spectroscopy was used to assess the effects of adsorbates on the structures of the metal cluster frames after they had been decarbonylated. N_2, H_2, or propene flowed through and around the catalyst loaded in the EXAFS cell at 298 K and 1 bar, while EXAFS spectra were recorded. Representative data, showing the goodness of the fits, are presented in Figures 1–3. The EXAFS parameters characterizing the catalysts in N_2 at 298 K and 1 bar (Table 4a) are in excellent agreement with those characterizing the decarbonylated samples at liquid nitrogen temperature and under vacuum (Table 2). These results show that the samples were stable at room temperature and had not been oxidized by adventitious air in the handling.

The EXAFS parameters characterizing the samples in H_2 and in propene (Tables 4b, 4c) also show essentially unchanged metal frames, as indicated by the Ir–Ir coordination

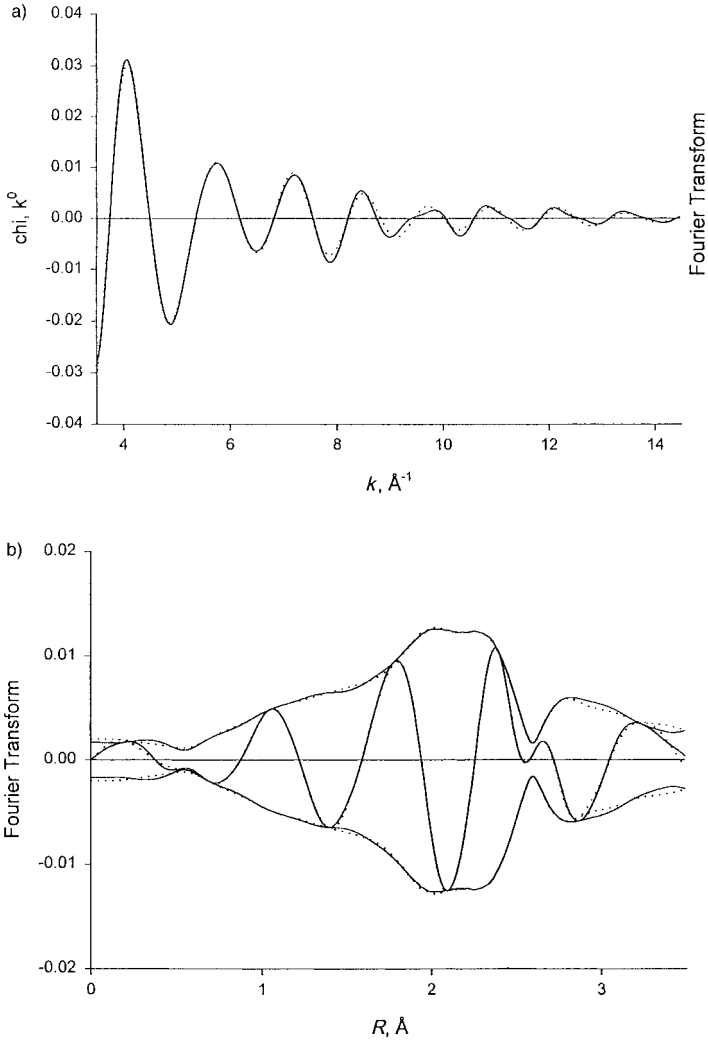

Figure 1. Results of analysis of Ir L_{III} edge EXAFS data obtained with the best calculated coordination parameters characterizing the γ-Al_2O_3-supported Ir_4 under N_2 flow at 298 K: a) experimental EXAFS function (solid line) and sum of the calculated Ir–Ir + Ir–O_s + Ir–O_l + Ir–Al contributions (dashed line); b) imaginary part and magnitude of uncorrected Fourier transform (k^0 weighted) of experimental EXAFS (solid line) and sum of the calculated Ir–Ir + Ir–O_s + Ir–O_l + Ir–Al contributions (dashed line; Ir–O_s = short and Ir–O_l = long Ir–O contribution).

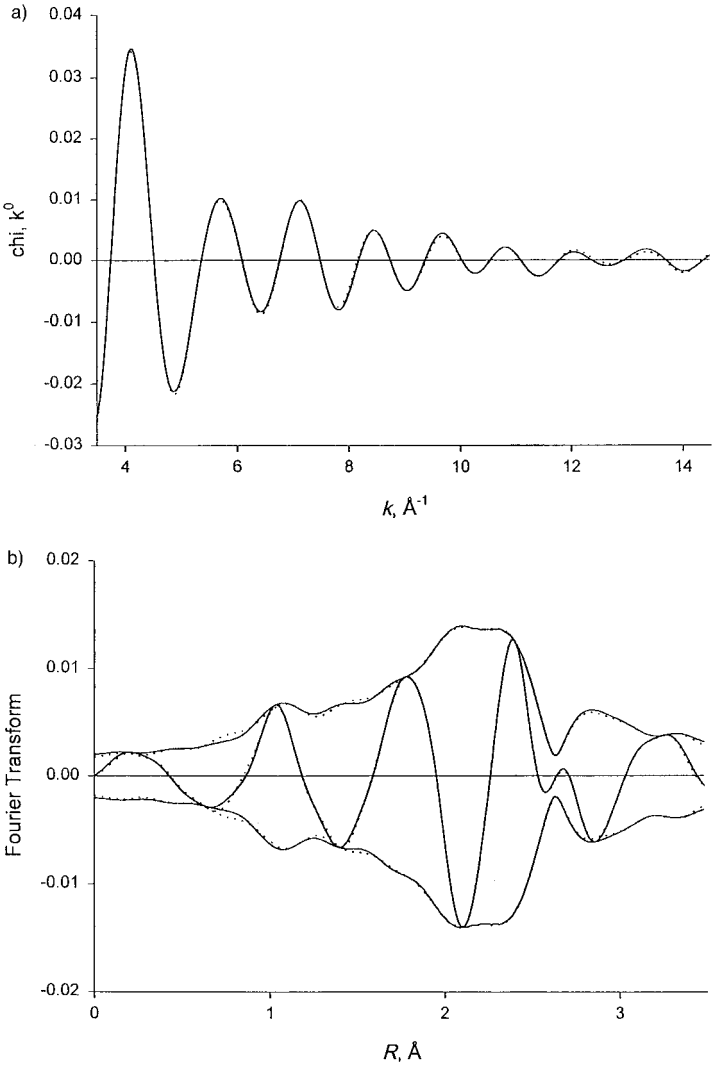

Figure 2. Results of analysis of Ir L_{III} edge EXAFS data obtained with the best calculated coordination parameters characterizing the γ-Al_2O_3-supported Ir_6 under N_2 flow at 298 K: a) experimental EXAFS function (solid line) and sum of the calculated Ir–Ir + Ir–O_s + Ir–O_l + Ir–Al contributions (dashed line); b) imaginary part and magnitude of uncorrected Fourier transform (k^0 weighted) of experimental EXAFS (solid line) and sum of the calculated Ir–Ir + Ir–O_s + Ir–O_l + Ir–Al contributions (dashed line).

numbers and distances, but there is a suggestion that the Ir–Ir distances of the Ir_4 clusters in H_2 might have increased slightly relative to the values for the clusters in N_2; however, the apparent changes in this distance are not distinguishable from the experimental uncertainty, which is estimated to be ± 0.05 Å.

The data characterizing the metal-support interfaces in these samples do not show the same consistency as those characterizing the metal frames, and this result is expected, being an indication of the relatively large experimental uncertainty in these parameters; the errors in the metal-oxygen coordination numbers are estimated to be roughly $\pm 50\,\%$.[13]

EXAFS spectra of working catalysts: When propene and H_2 flowed together through the cell containing each of the catalysts, catalytic hydrogenation occurred as shown by

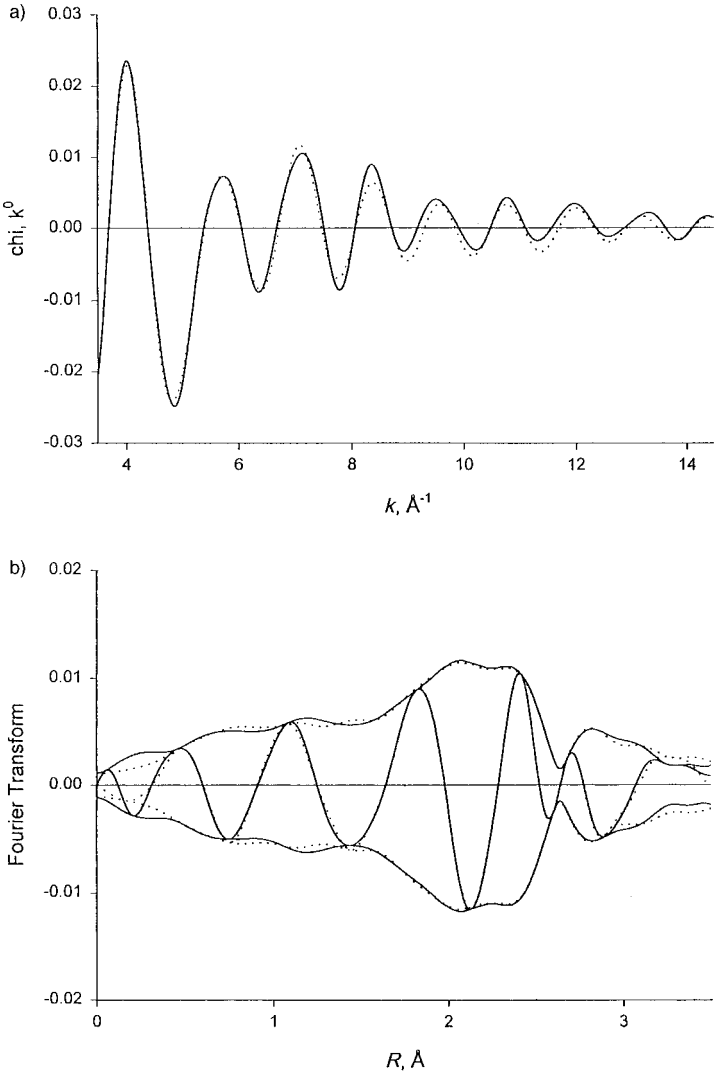

Figure 3. Results of analysis of Ir L_{III} edge EXAFS data obtained with the best calculated coordination parameters characterizing the MgO-supported Ir_4 under N_2 flow at 298 K: a) experimental EXAFS function (solid line) and sum of the calculated Ir–Ir + Ir–O_s + Ir–O_l contributions (dashed line); b) imaginary part and magnitude of uncorrected Fourier transform (k^0 weighted) of experimental EXAFS (solid line) and sum of the calculated Ir–Ir + Ir–O_s + Ir–O_l contributions (dashed line).

product analyses, which indicated the presence of propane (Table 5). Steady-state operation was obtained after 2 h on stream in the flow reactor, and propene conversions ranged from 28 to 52 %. These data show that the EXAFS parameters provide evidence of the structures of working catalysts in atmospheres predominantly containing the reactants H_2 and propene. The EXAFS data (Table 6, see page 2422) show that the metal frames of the working catalysts were not significantly different from those characterizing the catalysts in N_2, H_2, or propene.

Discussion

Identification of the supported clusters as catalytically active species: The EXAFS data show that each of the metal-oxide-supported clusters investigated here was the only detected noble-metal species present in inert N_2, in H_2, in propene, and in mixtures of H_2 and propene undergoing catalytic hydrogenation. Thus, the clusters themselves, on more than one kind of support (Ir_4/γ-Al_2O_3, Ir_6/γ-Al_2O_3, and Ir_4/MgO), are inferred to be stable in the various atmospheres at 298 K and to be the catalytically active species for propene hydrogenation.

One might question whether these results could be explained instead in terms of catalysis by some small minority species in the catalysts, such as larger clusters or particles of iridium. We tend to rule out this explanation in view of the mild conditions of the experiments, carried out at much lower temperatures than those at which substantial sintering of the iridium has been observed,[1] and in view of the systematic trend towards increased catalytic activity of the iridium for toluene hydrogenation when similar samples were treated at successively higher temperatures in H_2 to cause various degrees of sintering;[14–16] the results show that there was a smooth increase in catalytic activity with increasing average cluster or particle size in the catalysts consisting of aggregated iridium.[16] Thus, the data confirm the implicit assumption of earlier work[15] in which conclusions were drawn about the effects of cluster size[16] and support[17] on the catalytic activity for toluene hydrogenation. Suggestions have been made

Table 4a. EXAFS results characterizing structural parameters of supported metal clusters during varying conditions at 298 K and 1 bar.[a]

Catalyst modeled as	Conditions during scan			EXAFS parameters					
	$p_{propene}$ [bar]	$p_{hydrogen}$ [bar]	$p_{nitrogen}$ [bar]	Shell	N	R [Å]	$10^3 \times \Delta\sigma^2$ [Å^2]	ΔE_0 [eV]	EXAFS reference
Ir_4/γ-Al_2O_3	0	0	1.00	Ir–Ir	3.2	2.67	4.5	– 0.9	Pt–Pt
				Ir–$O_{support}$					
				Ir–O_s	1.3	2.17	3.5	– 15.0	Pt–O
				Ir–O_l	0.5	2.69	– 4.6	– 11.2	Pt–O
				Ir–Al	0.3	1.78	8.2	7.2	Ir–Al
Ir_6/γ-Al_2O_3	0	0	1.00	Ir–Ir	3.9	2.70	4.4	– 3.8	Pt–Pt
				Ir–$O_{support}$					
				Ir–O_s	1.3	2.26	4.2	– 20.0	Pt–O
				Ir–O_l	0.8	2.72	– 4.2	– 13.1	Pt–O
				Ir–Al	0.1	1.46	– 5.2	12.7	Ir–Al
Ir_4/MgO	0	0	1.00	Ir–Ir	3.0	2.67	4.5	– 0.9	Pt–Pt
				Ir–$O_{support}$					
				Ir–O_s	1.3	2.15	3.5	– 15.0	Pt–O
				Ir–O_l	0.5	2.69	– 4.6	– 11.2	Pt–O

[a] Notation as in Tables 2 and 3.

© WILEY-VCH Verlag GmbH, D-69451 Weinheim, 1999
0947-6539/99/0508-2420 $ 17.50+.50/0 *Chem. Eur. J.* **1999**, *5*, No. 8

Table 4b. EXAFS results characterizing structural parameters of supported metal clusters during varying conditions at 298 K and 1 bar.[a]

Catalyst modeled as	Conditions during scan $p_{propene}$ [bar]	$p_{hydrogen}$ [bar]	$p_{nitrogen}$ [bar]	EXAFS parameters Shell	N	R [Å]	$10^3 \times \Delta\sigma^2$ [Å^2]	ΔE_0 [eV]	EXAFS reference
Ir_4/γ-Al_2O_3	0	1.00	0	Ir–Ir	3.2	2.71	2.4	– 2.4	Pt–Pt
				Ir–$O_{support}$					
				Ir–O_s	1.3	2.17	3.5	– 15.6	Pt–O
				Ir–O_l	0.5	2.70	– 6.8	– 10.9	Pt–O
				Ir–Al	0.3	1.79	5.1	7.6	Ir–Al
Ir_6/γ-Al_2O_3	0	1.00	0	Ir–Ir	4.0	2.71	5.3	– 3.2	Pt–Pt
				Ir–$O_{support}$					
				Ir–O_s	1.3	2.23	1.2	– 18.3	Pt–O
				Ir–O_l	0.5	2.72	– 5.2	– 13.0	Pt–O
				Ir–Al	0.1	1.51	– 0.8	3.7	Ir–Al
Ir_4/MgO	0	1.00	0	Ir–Ir	2.9	2.70	1.4	– 1.2	Pt–Pt
				Ir–$O_{support}$					
				Ir–O_s	1.3	2.15	2.0	– 12.7	Pt–O
				Ir–O_l	0.5	2.69	– 6.3	– 9.9	Pt–O

[a] Notation as in Tables 2 and 3.

Table 4c. EXAFS results characterizing structural parameters of supported metal clusters during varying conditions at 298 K and 1 bar.[a]

Catalyst modeled as	Conditions during scan $p_{propene}$ [bar]	$p_{hydrogen}$ [bar]	$p_{nitrogen}$ [bar]	EXAFS parameters Shell	N	R [Å]	$10^3 \times \Delta\sigma^2$ [Å^2]	ΔE_0 [eV]	EXAFS reference
Ir_4/γ-Al_2O_3	1.00	0	0	Ir–Ir	3.1	2.70	2.6	– 2.8	Pt–Pt
				Ir–$O_{support}$					
				Ir–O_s	1.3	2.17	3.5	– 15.6	Pt–O
				Ir–O_l	0.5	2.70	– 6.8	– 10.9	Pt–O
				Ir–Al	0.2	1.73	4.5	9.2	Ir–Al
Ir_6/γ-Al_2O_3	1.00	0	0	Ir–Ir	4.1	2.70	4.5	– 0.8	Pt–Pt
				Ir–$O_{support}$					
				Ir–O_s	1.0	2.21	– 1.0	– 10.4	Pt–O
				Ir–O_l	0.8	2.70	– 2.2	– 15.3	Pt–O
				Ir–Al	0.3	1.59	15.0	– 14.0	Ir–Al
Ir_4/MgO	1.00	0	0	Ir–Ir	3.2	2.71	2.9	– 2.8	Pt–Pt
				Ir–$O_{support}$					
				Ir–O_s	1.5	2.15	2.0	– 9.8	Pt–O
				Ir–O_l	0.5	2.69	– 6.3	– 9.9	Pt–O

[a] Notation as in Tables 2 and 3.

elsewhere[15, 18] about the possible causes of the cluster size effect on the activity, and the issues are unresolved.

The lack of significant changes in the cluster frames (approximated as tetrahedral Ir_4 and octahedral Ir_6) in the presence of reactants alone or in combination confirms the robustness of these metal frames. We infer that the reactants provided ligands that were adsorbed on the clusters; the evidence is as follows: the metal–metal distances in the

Table 5. EXAFS structural parameters of supported metal clusters during propene hydrogenation catalysis at 298 K and 1 bar.[a]

Catalyst modeled as	Conditions during scan $p_{propene}$ [bar]	$p_{hydrogen}$ [bar]	$p_{nitrogen}$ [bar]	EXAFS parameters Shell	N	R [Å]	$10^3 \times \Delta\sigma^2$ [Å^2]	ΔE_0 [eV]	EXAFS reference
Ir_4/γ-Al_2O_3	0.50	0.50	0	Ir–Ir	3.2	2.71	2.4	– 3.2	Pt–Pt
				Ir–$O_{support}$					
				Ir–O_s	1.3	2.17	3.5	– 15.6	Pt–O
				Ir–O_l	0.5	2.70	– 6.8	– 10.9	Pt–O
				Ir–Al	0.3	1.77	9.3	2.6	Ir–Al
Ir_6/γ-Al_2O_3	0.50	0.50	0	Ir–Ir	4.0	2.71	– 5.3	– 3.2	Pt–Pt
				Ir–$O_{support}$					
				Ir–O_s	1.3	2.23	1.2	– 18.3	Pt–O
				Ir–O_l	0.5	2.72	5.2	– 13.0	Pt–O
				Ir–Al	0.1	1.51	0.6	– 3.7	Ir–Al
Ir_4/MgO	0.50	0.50	0	Ir–Ir	3.0	2.72	1.5	– 2.5	Pt–Pt
				Ir–$O_{support}$					
				Ir–O_s	1.3	2.15	2.0	– 12.7	Pt–O
				Ir–O_l	0.5	2.69	– 6.3	– 9.9	Pt–O

[a] Notation as in Tables 2 and 3.

Table 6. Propene hydrogenation catalyzed by supported metal clusters at 298 K and 1 bar.

Catalyst modeled as	$p_{propene}$ [bar]	$p_{hydrogen}$ [bar]	Propene conversion
Ir_4/γ-Al_2O_3	0.50	0.50	0.45
Ir_6/γ-Al_2O_3	0.50	0.50	0.54
Ir_4/MgO	0.50	0.50	0.28

supported clusters measured by EXAFS spectroscopy in the presence of H_2, propene, and mixtures of H_2 + propene are all within the range of 2.67 to 2.72 Å (Table 4). These Ir–Ir distances are indistinguishable within the experimental uncertainty from those of (crystalline) iridium clusters saturated with ligands, for example, $[Ir_4(CO)_{12}]$ (2.69 Å) and $[Ir_6(CO)_{16}]$ (2.77 Å); the former value was determined both by X-ray diffraction[10] and by EXAFS spectroscopy,[1] as was the latter.[19, 20]

The implication of the comparison is that the clusters in the presence of H_2, propene, and mixtures of H_2 + propene had a substantial number of coordinated ligands. However, theoretical calculations by density functional methods have shown that Ir_4 clusters supported on zeolite NaY have essentially this same distance when only a single carbon or hydrogen ligand is present in addition to the support.[18] Thus, the Ir–Ir distances observed in the present work are in accord with related reports indicating the presence of ligands on the clusters, but they are not sufficient to determine how many ligands were present or whether the supported clusters were coordinatively saturated. (The EXAFS parameters characterizing the Ir-low-Z contributions do not shed additional light on the ligands because of the relatively large uncertainties in the metal-low-Z coordination numbers and the inability of the EXAFS spectroscopy to distinguish between low-Z scatterers such as oxygen and carbon.)

The theoretically determined Ir–Ir distance in free Ir_4 is only about 2.5 Å.[18] This result, combined with the theoretical result that the effect of the zeolite support, modeled as a six-ring, is to increase the Ir–Ir distance by only a few hundredths of an Ångstrom unit, leads to a question about the Ir–Ir distances of the supported clusters under vacuum (Table 3); these are 2.67 and 2.68 Å and are much closer to the values characterizing the ligated clusters than to the theoretical value characterizing the clusters without ligands other than the zeolite support. We suggest that a possible explanation for the apparent discrepancy is that the clusters formed by decarbonylation from the precursor metal carbonyls were not entirely free of ligands besides the support; for example, carbon might have remained on the metal, as has been suggested before.[14]

These results are contrasted with those of Vaarkamp et al.,[21] who investigated platinum clusters or particles in zeolite HLTL. The clusters or particles had a distribution of sizes, with an average of about 13 atoms per cluster or particle; they were prepared from a metal salt, not a metal carbonyl. EXAFS data show that the chemisorption of hydrogen caused the average Pt–Pt distance to increase from 2.66 Å, for the sample under vacuum, to 2.74 Å, for the sample in H_2. The pattern of an increase in metal–metal distance upon treatment of an evacuated sample with H_2 is not in agreement with our data. A key difference between Vaarkamp's samples and ours (besides the difference in the metal) may be the temperature of sample treatment; treatment at a relatively high temperature in H_2, such as was done by Vaarkamp et al., would be expected to remove carbon ligands (remaining from CO ligands), whereas our relatively low-temperature treatments may not have removed these ligands. Thus, we postulate that our samples were not entirely ligand free.

There is a tradeoff here; the higher temperature treatment may produce cleaner samples, but it does so at the expense of structural uniformity (as the high-temperature treatments lead to aggregation of the metal).

Experimental Section

Methods and materials: All syntheses and sample transfers were performed with exclusion of air and moisture on a double-manifold Schlenk line and in a N_2-filled glovebox (AMO-2032, Vacuum Atmospheres). N_2, He, C_3H_6, and H_2 (Matheson, 99.999 %) were purified by passage through traps containing particles of Cu and activated zeolite to remove traces of O_2 and moisture, respectively. *n*-Pentane (Aldrich), used as a solvent, was refluxed under N_2 in the presence of Na/benzophenone ketyl to remove traces of water and deoxygenated by sparging with dry N_2 prior to use. $[Ir_4(CO)_{12}]$ (Strem, 99 %) and $[Ir(CO)_2(acac)]$ (dicarbonylacetylacetonato iridium(I), Strem, 99 %) were used as received. The γ-Al_2O_3 support was prepared by first forming a paste of porous γ-Al_2O_3 (Degussa, Aluminum Oxide C) and deionized water, followed by overnight drying at 393 K, calcination at 673 K in flowing O_2 (Matheson Extra Dry Grade) for 2 h, and evacuation at 10^{-3} Torr and the final temperature for 14 h. The BET surface area of the resultant material was measured to be about 100 $m^2 g^{-1}$. MgO (E.M. Science, 60 $m^2 g^{-1}$) was also calcined at 673 K followed by evacuation.

Synthesis of supported metal clusters: The γ-Al_2O_3- and MgO-supported samples were prepared by slurrying $[Ir_4(CO)_{12}]$ with the respective powder support in *n*-pentane under N_2 for 12 h at room temperature followed by overnight evacuation at 298 K to remove the solvent. $[Ir_4(CO)_{12}]$ was added in an amount sufficient to give samples containing 1 wt % Ir. Experimental details are as described by Alexeev et al.[1] and Maloney et al.[6].

The γ-Al_2O_3-supported $[Ir_6(CO)_{15}]^{2-}$ was prepared by adsorbing $[Ir(CO)_2(acac)]$ on the γ-Al_2O_3 support followed by room-temperature evacuation and the ensuing reductive carbonylation in CO at 373 K for 10 h. Details are described by Zhao et al.[2]. Room-temperature infrared spectra were recorded with samples in flowing He.

Decarbonylation of supported metal clusters: The samples were decarbonylated by treatment in flowing He as the temperature was ramped (3 K min^{-1}) from 25 K to the desired temperature and then held at that temperature for 2 h. Infrared spectra were recorded after the samples had been cooled to room temperature.

Infrared spectroscopy: Spectra were recorded with a Bruker IFS-66V spectrometer with a spectral resolution of 4 cm^{-1}. Samples were pressed into self-supporting wafers and mounted in the cell in the drybox.

EXAFS spectroscopy: EXAFS experiments were performed at X-ray beamline X-11A at the National Synchrotron Light Source (NSLS), Brookhaven National Laboratory, Upton, NY (USA). The storage ring at SSRL operated with an electron energy of 2.5 GeV; the ring current was 140–240 mA. All of the supported metal clusters were characterized by EXAFS spectroscopy after synthesis of the organometallic compounds and the decarbonylated counterparts. Experimental details are given elsewhere.[22]

A cell allowing flow through a packed bed of sample was constructed for in situ EXAFS experiments, allowing air-sensitive powder samples to be packed in a sealed cell and the X-ray beam to be transmitted through Kapton®-sealed windows. During in situ EXAFS experiments, gases (N_2, C_3H_6, and/or H_2) passed through the cell mounted in the beamline. The EXAFS data were recorded under various conditions of flow, while the temperature was maintained at 298 K.

© WILEY-VCH Verlag GmbH, D-69451 Weinheim, 1999
0947-6539/99/0508-2422 $ 17.50+.50/0 *Chem. Eur. J.* **1999**, *5*, No. 8

EXAFS reference data: The EXAFS reference data were determined with materials of known structure. The Ir–Ir and Ir–$O_{support}$ interactions were analyzed with phase shifts and backscattering amplitudes obtained from EXAFS data characterizing platinum foil and $Na_2Pt(OH)_6$, respectively. The Ir–C and Ir–O* contributions (O* is carbonyl oxygen) were analyzed with phase shifts and backscattering amplitudes obtained from EXAFS data characterizing crystalline $[Ir_4(CO)_{12}]$, which has only terminal CO ligands. The parameters used to extract these results from the EXAFS data are summarized in Table 1.

Propene hydrogenation catalysis: Data characterizing the hydrogenation of propene catalyzed by the supported metal clusters were obtained at the University of California in the same EXAFS cell that was used for the in situ EXAFS measurements at the synchrotron. The temperature was 298 K, and the pressure atmospheric; the adsorbate partial pressures were varied. The effluent gas mixture was analyzed with an on-line Hewlett–Packard gas chromatograph (HP-5890, Series II) equipped with a DB-624 capillary column (J. and W. Scientific) and flame ionization detector.

EXAFS data analysis: The EXAFS data were extracted from the spectra with the XDAP software.[23] The EXAFS function characterizing each sample was obtained from the X-ray absorption spectrum, as before.[24] The normalized EXAFS function characterizing each sample is the average of four scans. The main contributions to the spectra were isolated by inverse Fourier transformation of the final EXAFS function. The analysis was done with the Fourier-filtered data. The parameters characterizing both low-Z (Ir-O, Ir-C) and high-Z (Ir–Ir) contributions were determined by multiple-shell fitting in r space (where r is the distance from the absorbing atom, Ir) and in k space (k is the wave vector) with application of k^1 and k^3 weighting in the Fourier transformations. The raw EXAFS data at the Ir L_{III} edge were first Fourier transformed with a k^3 weighting over the range $2.75 < k < 14.5$ Å^{-1} without any phase correction. The Fourier transformed data were then inverse transformed in the range $0.1 < r < 3.5$ Å to isolate the main-shell contributions from low-frequency noise. With a difference file technique,[25] the Ir–Ir contributions in each sample, the largest in the EXAFS spectra, were first estimated and subsequently subtracted from the raw data. The difference file was expected to represent Ir–$O_{support}$ and Ir–CO* contributions. After optimizing the parameters for these two contributions, the first-guess Ir–Ir contributions were then added and compared with the raw data. The final parameters representing the high-Z (Ir–Ir) and low-Z (Ir–O and Ir–C) contributions were determined by multiple-shell fitting in r space and in k space with application of k^1 and k^3 weighting[13] over the range $3.6 < k < 14.5$ Å^{-1} and $0.1 < r < 3.5$ Å. The maximum number of free parameters used to fit the main-shell contributions was 20. The statistically justified number of free parameters (n), estimated from the Nyquist theorem,[24] $n = (2\Delta k \Delta r/\pi) + 1$, where Δk and Δr are the k and r ranges used to fit the data, was approximately 25.

Acknowledgment

The research was supported by the National Science Foundation (Grant CTS-9615257). We acknowledge the support of the U.S. Department of Energy, Division of Materials Sciences, under contract number DE-FG05-89ER45384, for its role in the operation and development of beam line X-11A at the National Synchrotron Light Source (NSLS). The NSLS is supported by the Department of Energy, Division of Materials Sciences and Division of Chemical Sciences, under Contract No. DE-AC02-76CH00016. X-Ray absorption data were analyzed with the XDAP software.[23]

[1] O. Alexeev, G. Panjabi, B. C. Gates, *J. Catal.* **1998**, *173*, 196.
[2] A. Zhao, B. C. Gates, *J. Am. Chem. Soc.* **1996**, *118*, 2458.
[3] B. C. Gates, *Chem. Rev.* **1995**, *95*, 511.
[4] R. Prins, D. C. Koningsberger, in *X-Ray Absorption: Principles, Applications, Techniques of EXAFS, SEXAFS and XANES*, (Eds.: D. C. Koningsberger, R. Prins), Wiley, New York, **1986**, p. 321.
[5] D. M. Adams, I. D. Taylor, *J. Chem. Soc. Faraday Trans. 2* **1982**, *78*, 1573.
[6] S. D. Maloney, F. B. M. Van Zon, M. J. Kelley, D. C. Koningsberger, B. C. Gates, *Catal. Lett.* **1990**, *5*, 161.
[7] B. C. Gates, *J. Mol. Catal.* **1994**, *86*, 95.
[8] D. Lu, J. J. Rehr, *J. Phys. (Paris) C8* **1986**, *47*, 67.
[9] F. B. M. Van Zon, S. D. Maloney, B. C. Gates, D. C. Koningsberger, *J. Am. Chem. Soc.* **1993**, *115*, 10317.
[10] M. R. Churchill, J. P. Hutchinson, *Inorg. Chem.* **1978**, *15*, 3528.
[11] R. Bau, M. Y. Chiang, C-Y. Wei, K. Garlaschelli, S. Martinengo, T. F. Koetzle, *Inorg. Chem.* **1984**, *23*, 4758.
[12] F. Demartin, M. Manassero, M. Sansoni, L. Garlaschelli, S. Martinengo, F. Canziani, *J. Chem. Soc. Chem. Commun.* **1980**, 903.
[13] J. B. A. D. Van Zon, D. C. Koningsberger, H. F. J. Van't Blik, D. E. Sayers, *J. Phys. Chem.* **1985**, *82*, 5742.
[14] O. Alexeev, B. C. Gates, *J. Catal.* **1998**, *176*, 310.
[15] B. C. Gates, in *Catalysis by Di- and Polynuclear Metal Cluster Complexes* (Eds.: R. D. Adams, F. A. Cotton), Wiley, New York, **1998**, pp. 403.
[16] F.-S. Xiao, W. A. Weber, O. Alexeev, B. C. Gates, *Stud. Surf. Sci. Catal. B* **1996**, *101*, 1135.
[17] Z. Xu, F.-S. Xiao, S. K. Purnell, O. Alexeev, S. Kawi, S. E. Deutsch, B. C. Gates, *Nature (London)* **1994**, *372*, 346.
[18] A. M. Ferrari, K. M. Neyman, M. Mayer, M. Staufer, B. C. Gates, N. Rösch, *J. Phys. Chem. B* **1999**, *103*, 5311.
[19] L. Garlaschelli, S. Martinengo, P. L. Bellon, F. Demartin, M. Manassero, M. Y. Chiang, C.-Y. Wei, R. Bau, *J. Am. Chem. Soc.* **1984**, *106*, 6664.
[20] S. Kawi, J.-R. Chang, B. C. Gates, *J. Am. Chem. Soc.* **1993**, *115*, 4830.
[21] M. Vaarkamp, B. L. Mojet, M. J. Kappers, J. T. Miller, D. C. Koningsberger, *J. Phys. Chem.* **1995**, *99*, 16067.
[22] R. E. Jentoft, S. E. Deutsch, B. C. Gates, *Rev. Sci. Instrum.* **1996**, *67*, 2111.
[23] M. Vaarkamp, J. C. Linders, D. C. Koningsberger, *Physica B* **1995**, *209*, 159.
[24] D. E. Sayers, B. A. Bunker, in *X-Ray Absorption: Principles, Applications, Techniques of EXAFS, SEXAFS and XANES*, (Eds.: D. C. Koningsberger, R. Prins), Wiley, New York, **1986**, p. 211.
[25] P. S. Kirlin, F. B. M. Van Zon, D. C. Koningsberger, B. C. Gates, *J. Phys. Chem.* **1990**, *94*, 8439.

Received: December 12, 1998 [F1497]